ELSEVIER

Chemistry & Biology 8 (2001) 1231–1237

Chemistry & Biology

www.elsevier.com/locate/chembiol

Research Paper

# Alternative oxidation by isopenicillin *N* synthase observed by X-ray diffraction

James M. Ogle [a,1], Ian J. Clifton [a], Peter J. Rutledge [a], Jonathan M. Elkins [a], Nicolai I. Burzlaff [a], Robert M. Adlington [a], Peter L. Roach [b,2], Jack E. Baldwin [a,*]

[a] *The Dyson Perrins Laboratory and the Oxford Centre for Molecular Sciences, University of Oxford, South Parks Road, Oxford OX1 3QY, UK*
[b] *Department of Chemistry, University of Southampton, Highfield, Southampton SO17 1BJ, UK*

Received 22 March 2001; revisions requested 26 September 2001; revisions received 26 September 2001; accepted 28 September 2001
First published online 7 November 2001

**Abstract**

**Background:** Isopenicillin *N* synthase (IPNS) catalyses formation of bicyclic isopenicillin *N*, precursor to all penicillin and cephalosporin antibiotics, from the linear tripeptide δ-(L-α-aminoadipoyl)-L-cysteinyl-D-valine. IPNS is a non-haem iron(II)-dependent enzyme which utilises the full oxidising potential of molecular oxygen in catalysing the bicyclisation reaction. The reaction mechanism is believed to involve initial formation of the β-lactam ring (via a thioaldehyde intermediate) to give an iron(IV)-oxo species, which then mediates closure of the 5-membered thiazolidine ring.

**Results:** Here we report experiments employing time-resolved crystallography to observe turnover of an isosteric substrate analogue designed to intercept the catalytic pathway at an early stage. Reaction in the crystalline enzyme–substrate complex was initiated by the application of high-pressure oxygen, and subsequent flash freezing allowed an oxygenated product to be trapped, bound at the iron centre. A mechanism for formation of the observed thiocarboxylate product is proposed.

**Conclusions:** In the absence of its natural reaction partner (the N–H proton of the L-cysteinyl-D-valine amide bond), the proposed hydroperoxide intermediate appears to attack the putative thioaldehyde species directly. These results shed light on the events preceding β-lactam closure in the IPNS reaction cycle, and enhance our understanding of the mechanism for reaction of the enzyme with its natural substrate. © 2001 Published by Elsevier Science Ltd.

**Keywords:** Enzymic oxidation; High-pressure oxygen; Non-haem iron enzyme; Penicillin biosynthesis; Time-resolved crystallography

## 1. Introduction

The desaturative bicyclisation of δ-(L-α-aminoadipoyl)-L-cysteinyl-D-valine (ACV) to isopenicillin *N* (IPN) is coupled to the reduction of dioxygen to water [1]. A mechanism has been proposed [2–4] wherein the two rings of IPN are closed sequentially, initial β-lactam formation giving rise to a reactive iron(IV)-oxo species which then mediates thiazolidine ring closure (Fig. 1a). Isopenicillin *N* synthase (IPNS) has been the subject of extensive mechanistic investigation [5], and crystal structures of Mn(II)-substituted IPNS [6] and of the anaerobic substrate complexes IPNS:Fe(II):ACV and IPNS:Fe(II):ACV:NO (incorporating nitric oxide as a dioxygen analogue) have been determined [3].

In order to use X-ray crystallography to investigate a transient species in an enzymatic reaction pathway, the intermediate must be present in high occupancy during the time required for data collection. This condition can be met if the reaction is initiated in a uniform and synchronous manner throughout the crystal, then either fast data collection methods such as Laue crystallography are used, or the lifetime of intermediates is extended, for which a variety of trapping strategies are available [7,8]. For the study of IPNS in this laboratory, techniques have been developed to initiate reaction in the crystalline state at room temperature by the application of high-pressure

[1] Present address: M.R.C. Laboratory of Molecular Biology, Hills Road, Cambridge CB2 2QH, UK.
[2] Also corresponding author.

* Corresponding author.
*E-mail addresses:* p.l.roach@soton.ac.uk (P.L. Roach), jack.baldwin@chem.ox.ac.uk (J.E. Baldwin).

1074-5521/01/$ – see front matter © 2001 Published by Elsevier Science Ltd.
PII: S1074-5521(01)00090-4

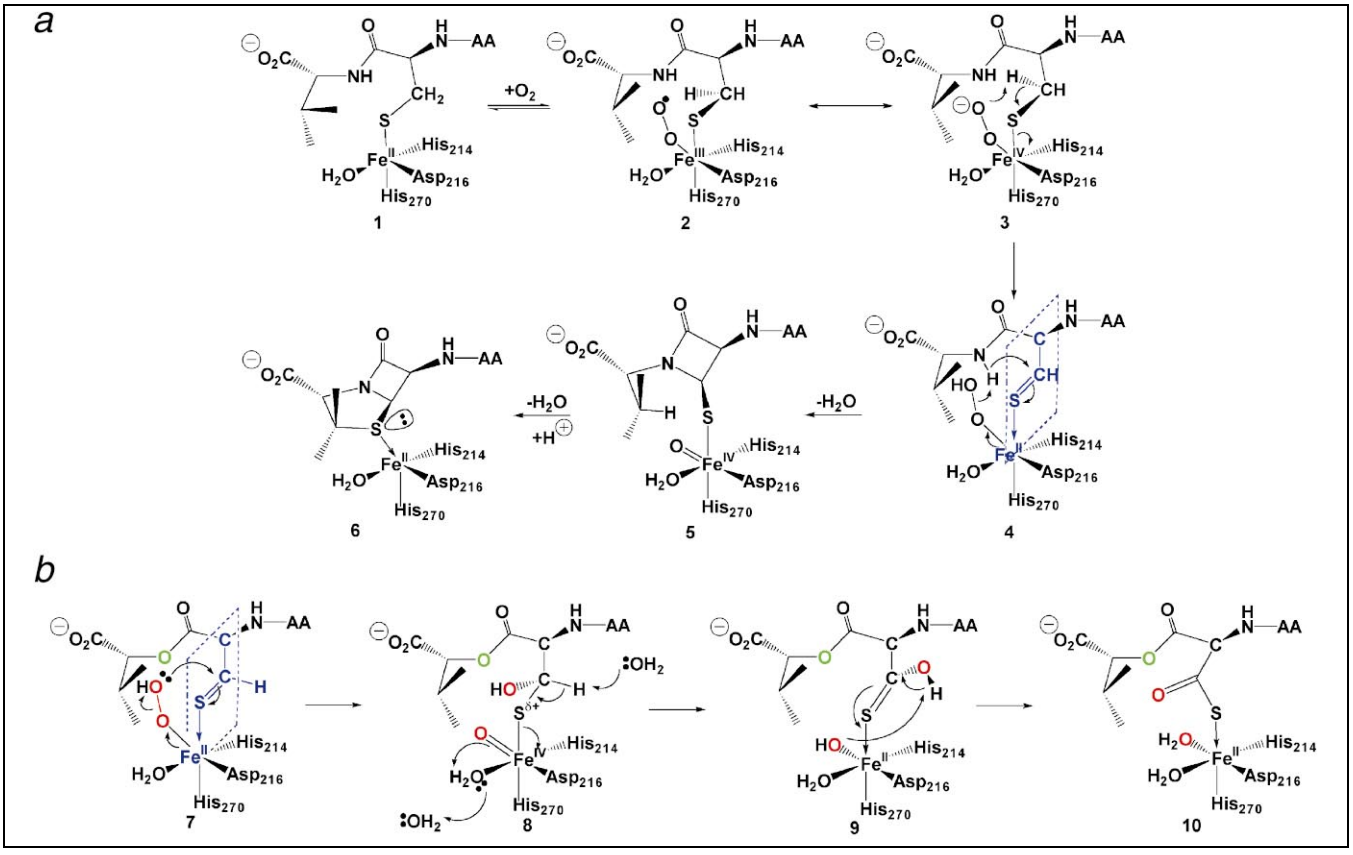


Fig. 1. Mechanisms for the reaction of IPNS with ACV and AC*O*V. (a) Proposed mechanism for the reaction of IPNS with its natural substrate ACV [3]. (b) Proposed pathway for generation of the thiocarboxylate product from the substrate analogue AC*O*V. See text for details of compounds **1**–**10**. AA, δ-(L-α-aminoadipoyl).

oxygen [4] (and a similar approach has subsequently been reported for application to the study of cytochrome $P_{450}$ [9]). Using a purpose-built device, anaerobically grown [10] crystals of IPNS, iron(II) and substrate (or substrate analogues) can be subjected to oxygen pressures of up to 60 bar. After a suitable reaction time, turnover is quenched by flash freezing in liquid nitrogen and data can be collected by conventional monochromatic X-ray diffraction techniques. This approach has recently allowed the structure of the natural enzyme–product complex to be determined, from crystals that initially contained the IPNS:Fe(II):ACV complex [4]. Furthermore, using a modified substrate and a strategy of combined chemical and cryogenic trapping, the structure of an iron-bound monocyclic β-lactam species was elucidated [4].

The results presented herein were obtained from the application of this approach to crystals incorporating the substrate analogue δ-(L-α-aminoadipoyl)-L-cysteine D-α-hydroxyisovaleryl ester (AC*O*V). AC*O*V is isosteric to the natural substrate, differing only in that the amide linkage to the C-terminal D-valine is replaced by an ester group. Deprotonation of that amide nitrogen by an iron-bound hydroperoxide is thought to be central to β-lactam formation (Fig. 1a) [3]. It was envisaged that crystallisation and oxygen-dependent turnover of IPNS with this substrate analogue would provide information on events occurring immediately prior to β-lactam closure during turnover of the natural substrate. The structures obtained indicate that cleavage of the hydroperoxide follows an alternative path when it is deprived of its natural reaction partner, the amide proton of the L-cysteinyl-D-valine link (Fig. 1b).

## 2. Results and discussion

### 2.1. The structure of the anaerobic enzyme–substrate analogue complex

The crystal structure of the anaerobic IPNS:Fe(II):AC*O*V complex was determined at 1.55 Å resolution (Fig. 2a). AC*O*V binds in an identical fashion to that seen for the natural substrate ACV [3]. The ester group adopts a *transoid* conformation in which the D-α-hydroxyisovaleryl $C_\alpha$-$O_\alpha$ bond lies in the plane of the L-cysteine-derived ester carbonyl group, mimicking a *trans* amide. The iron atom is pentacoordinate, with the three ligands derived from the protein, His 214, Asp 216 and His 270, and a single aquo ligand (Wat 401; key equivalent water molecules have been numbered consistently in all structures for clarity).

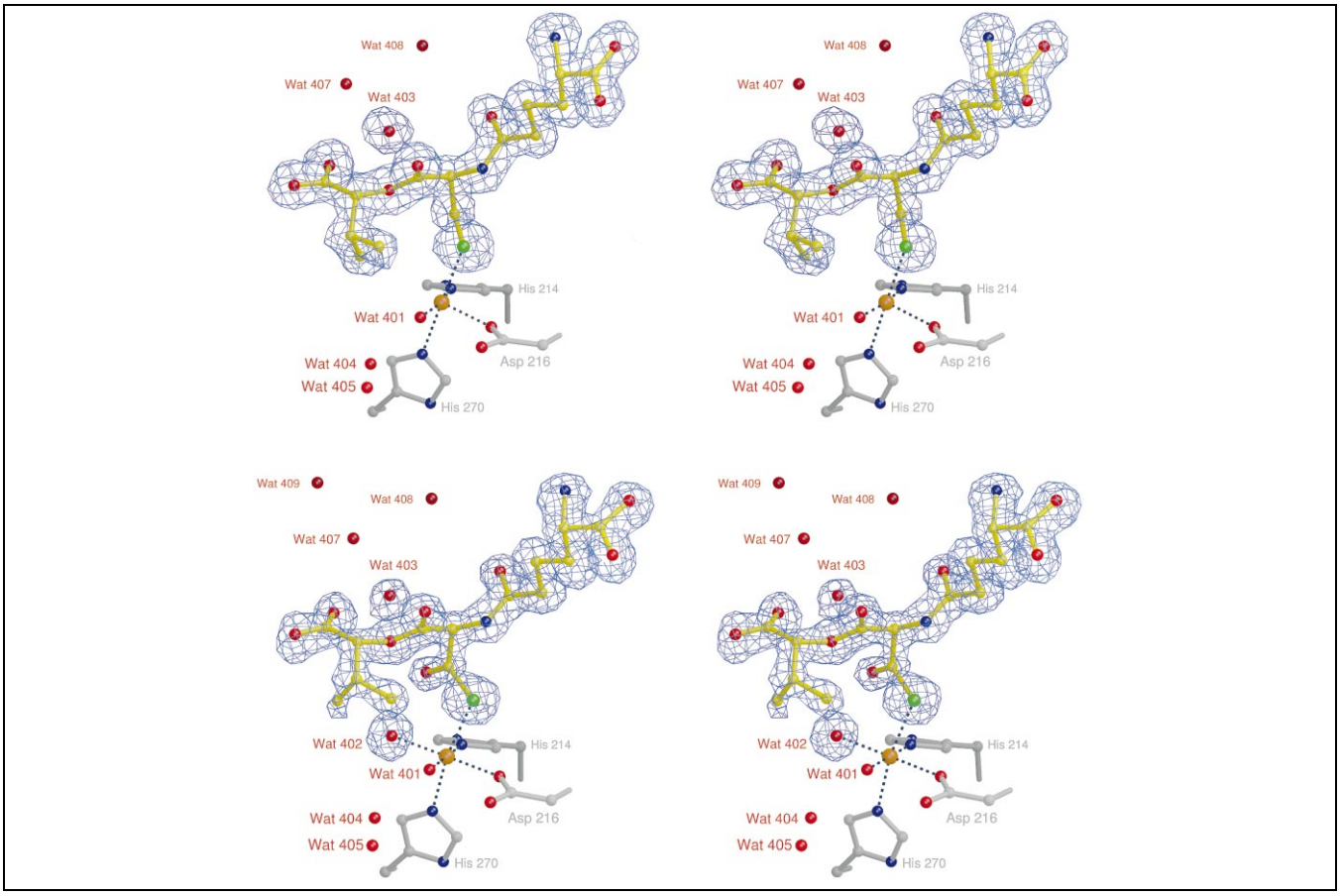


Fig. 2. Active site region of the complex IPNS:Fe(II):AC*O*V before and after exposure to oxygen. Stereo pictures of the X-ray crystal structures showing changes occurring in the active site region upon exposure to high-pressure oxygen. All electron density maps are ($2mF_{obs}-DF_{calc}$) maps and contoured at 1σ. (a) The IPNS:Fe(II):AC*O*V complex before exposure to oxygen, showing the substrate, protein ligands at iron, relevant water molecules and the vacant dioxygen coordination site. (b) Structure of an IPNS:Fe(II):AC*O*V crystal after 30 s exposure to 40 bar oxygen to 1.30 Å resolution, showing the presence of an additional aquo ligand *trans* to Asp 216, and density that corresponds to a thiocarboxylate species at the L-cysteinyl β-carbon.

As in the structure of IPNS:Fe(II):ACV, the proposed oxygen binding site *trans* to Asp 216 [3] is occupied by the isopropyl side chain of the substrate, which sits in van der Waals contact with the metal. The positions of amino acid side chains and adjacent water molecules in the vicinity of the active site correspond directly to those seen in the IPNS:Fe(II):ACV structure.

### 2.2. *The structure of a new IPNS–product complex*

Following the general technique [4] anaerobically grown crystals of IPNS:Fe(II):AC*O*V were subjected to high oxygen pressures for a range of time periods then rapidly frozen. In our previous studies, enzyme–product complexes generated from IPNS:Fe(II):substrate crystals were observed after relatively long reaction times, 10 min for the monocyclic β-lactam sulphoxide and 320 min in the case of the product IPN [4]. In contrast, exposure of crystals containing AC*O*V for times longer than 120 s led to disordered structures, presumably a result of product dissociation. However three crystals of IPNS:Fe(II):AC*O*V exposed to oxygen at 40 bar for much shorter times, two for 30 s and a third for 120 s, gave rise to well defined structures, determined to resolutions of 1.30, 1.40 and 1.50 Å, respectively. Each of these structures reveals electron density in the active site region that is best interpreted as a thiocarboxylate derivative of AC*O*V ligated to hexacoordinate iron (Fig. 2b).

In the complex of IPNS with its natural product IPN [4], the sulphur atom is seen to have migrated around the iron atom in the course of product formation. In contrast the sulphur atom of the product arising from AC*O*V occupies the same position as in the anaerobic complex (Fig. 3). The carbon atom adjacent to sulphur has however moved 0.66 Å with respect to the anaerobic reference structure, into close proximity to additional electron density which can be assigned to the oxygen atom of a thiocarboxylate (Fig. 2b). Electron density, attributable to a second aquo ligand (Wat 402), is also apparent in all three exposed structures, occupying the site *trans* to Asp 216. Such a ligand is absent from the product complex of IPNS with IPN [4] in which iron is pentacoordinate; in the com-

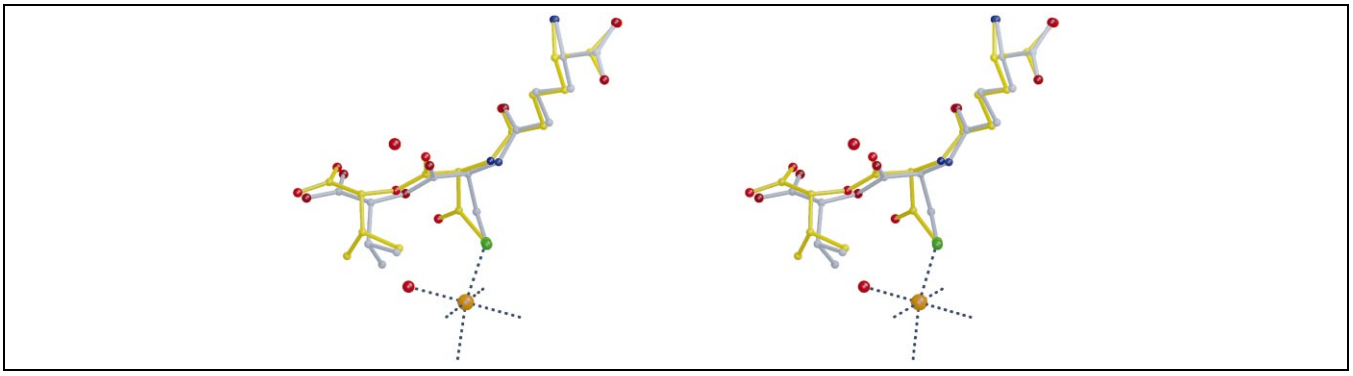

Fig. 3. The exposed and unexposed IPNS:Fe(II):AC*O*V structures overlaid. Stereo views of the exposed and unexposed structures overlaid to show changes in atomic positions occurring upon oxidation; unexposed IPNS:Fe(II):AC*O*V in lilac, 1.30 Å exposed IPNS:Fe(II):AC*O*V in yellow. Orientations of the other ligands at iron are indicated.

plex of Fe-IPNS with the monocyclic β-lactam sulphoxide, the oxygen of the sulphoxide coordinates to iron in this binding site [4]. It is likely that both this sulphoxide oxygen and Wat 402 in the exposed AC*O*V structures derive directly from molecular oxygen. The isopropyl group of AC*O*V has undergone a rotation of ca. 30°, moving away from the metal to accommodate the new water ligand opposite Asp 216 (Fig. 3). In doing so, it takes up a similar position to that seen for the isopropyl group of ACV in the IPNS:Fe(II):ACV:NO structure [3].

The thiocarboxylate oxygen atom is 2.77 Å from ligand Wat 402, ideally placed to form a hydrogen bonded six-membered ring involving the oxygen atom and one hydrogen of Wat 402, the three atoms of the thiocarboxylate functionality and the iron (Fig. 4). It is also possible to envisage a long hydrogen bond (3.22 Å) between the thiocarboxylate oxygen and a water molecule Wat 403. This water molecule lies in the plane defined by the three atoms of the thiocarboxylate group (Fig. 4a).

### *2.3. A mechanism for thiocarboxylate formation*

A thiocarboxylate product has previously been observed in transformation experiments with IPNS [11]. Reaction of the tripeptide substrate analogue δ-(L-α-aminoadipoyl)-L-β,β-difluorohomocysteinyl-D-valine (in which the L-cysteinyl residue of the natural substrate is replaced with L-β,β-difluorohomocysteine) with IPNS yielded a thiocarboxylate product. In that case the product was believed to form via a monocyclic γ-lactam intermediate. Such a mechanism cannot feasibly operate during the oxidation of AC*O*V. Thus we propose an alternative mechanism for the generation of the thiocarboxylate-containing species from AC*O*V (Fig. 1b).

In the mechanism proposed for the natural substrate (Fig. 1a) [3], the ACV thiolate displaces Gln 330 from the iron to form the pentacoordinate complex **1**. Thiolate binding initiates the reaction cycle by decreasing the Fe(II)/Fe(III) redox potential [12,13] and allowing oxygen to coordinate in the site *trans* to Asp 216, giving **2**. The binding of oxygen also forces a rotation of the valine isopropyl group by ca. 30°. Bound oxygen, as the superoxo species in **3**, selectively abstracts the *pro*-3*S* hydrogen from the L-cysteinyl β-carbon to form the thioaldehyde intermediate **4**. Cleavage of the hydroperoxide results in deprotonation of the amide, presumably via an initial hydrogen bond, followed by attack of the amide nitrogen on the thioaldehyde. This closes the β-lactam ring while also yielding one water molecule and the reactive iron(IV)-oxo species **5**, proposed mediator of the subsequent thiazolidine ring closure leading to **6**. During cyclisation of ACV, the thiolate sulphur ligand functions as a conductor for the flow of electrons from the substrate through the iron to dioxygen.

A similar sequence of events is probable with AC*O*V, to the point at which an analogous thioaldehyde **7** is generated (Fig. 1b). However, abstraction of an amide proton to form a strongly nucleophilic nitrogen is not possible with this ester analogue. Instead, the hydroperoxide itself could act as a nucleophile toward the thioaldehyde. If this occurs with concomitant cleavage of hydroperoxide, the distal oxygen atom would become incorporated in the product, bound to the L-cysteinyl β-carbon, and an iron-(IV)-oxo species **8** would be generated. In reaction of the natural substrate, closure of the β-lactam ring would force further rotation of the isopropyl group and bring the β-hydrogen of D-valine closer to the iron(IV)-oxo species, enabling the two to react to form the thiazolidine. Without this natural reaction partner near the iron(IV)-oxo moiety, further oxidation could occur at the L-cysteinyl-derived β-carbon instead, with the sulphur again acting as a conductor for the flow of electrons. The highly electron-deficient iron(IV) would cause strong positive polarisation of the sulphur, which could be stabilised by the transfer of two electrons to the metal with concomitant removal of the remaining proton from the L-cysteinyl β-carbon, forming a $C_\beta = S$ double bond and the iron(II)-thiocarboxylic acid species **9**. The second hydrogen atom on the L-cysteinyl β-carbon would therefore be of increased acidity, and there appear to be two plausible candidates to accept this pro-

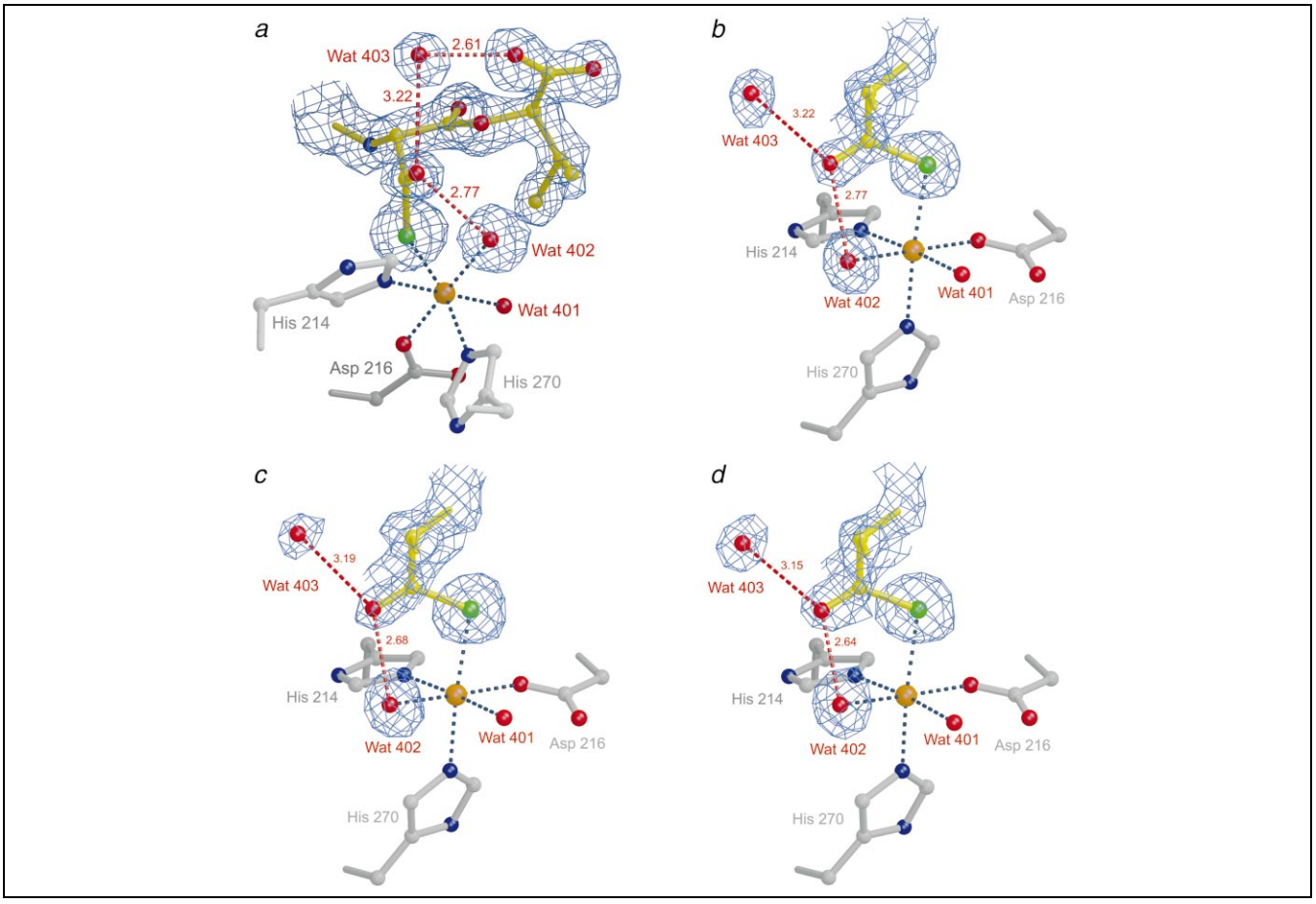


Fig. 4. Potential hydrogen bonding interactions in the active site region of the exposed IPNS:Fe(II):AC*O*V structure. The three exposed structures oriented to show the potential for hydrogen bonding around the thiocarboxylate oxygen, and to demonstrate the consistency of the thiocarboxylate electron density across the three structures. (a) From the 1.30 Å resolution structure in the plane of the thiocarboxylate, showing distances to Wat 402 and Wat 403. (b) The 1.30 Å 30 s, (c) the 1.40 Å 30 s, and (d) the 1.50 Å 120 s structures from an alternative angle.

ton: the water molecule Wat 403 (as shown in Fig. 1b), and the oxo ligand at iron(IV). Wat 403 is in good position relative to the hydrogen atom in question (it sits ca. 3.0–3.5 Å away, estimated from the position of this water in the product structure) and were it to act as the base, the proton could then be passed to the surface of the protein by a series of further water molecules (Wat 407, Wat 408 and Wat 409; Fig. 2b. It is through this channel that water molecules formed during the reaction of ACV are proposed to leave the active site [3].) Alternatively, the oxo ligand at iron(IV) could act as the required base. However this oxygen atom is further away from the proton in question (ca. 4.0–4.5 Å, based on the position of Wat 402 in the product structure), and it could instead receive a proton from the adjacent aquo ligand Wat 401, which could in turn equilibrate with water on the surface of the protein via a number of proton-transferring groups (Wat 404, Wat 405, and Wat 406; Asp 216, Asn 252 and Asp 215 side chains). Finally, in a tautomerisation step, a second proton could be transferred to the resulting hydroxo ligand from the thiocarboxylic acid in **9**, to yield a thiocarboxylate and the additional ligand Wat 402 bound to iron in **10**.

### *2.4. Significance*

The active site of IPNS is structurally related to a number of mononuclear non-haem iron-enzymes, which perform a wide range of chemical transformations, for example bacterial proline hydroxylase (Hsueh et al., personal communication), deacetoxycephalosporin C synthase [14], clavaminic acid synthase [15] and 4-hydroxyphenylpyruvate dioxygenase [16]. These enzymes share the so-called '2-His-1-carboxylate' facial triad of ligands around iron [12] and basic elements of oxygen activation chemistry. Variation in catalytic specificity must be achieved by fine-tuning of individual active site properties [12,13].

IPNS has previously demonstrated a remarkable range of substrate specificity and intriguing chemical versatility in transformation experiments [5]. The crystal structures observed here reveal the immediate result of a monooxygenase mode of activity, whereby one oxygen atom is incorporated into AC*O*V at a methylene carbon and the other is reduced to water. This stands in contrast to the oxidase type activity with ACV, in which dioxygen is re-

Table 1
Data collection and statistics: all crystals of IPNS:Fe(II):AC*O*V

| Exposure to oxygen | unexposed | | 40 bar, 30 s | | 40 bar, 30 s | | 40 bar, 120 s | |
|---|---|---|---|---|---|---|---|---|
| X-ray source | ID14-3 ESRF | | ID14-4 ESRF | | ID14-4 ESRF | | ID14-3 ESRF | |
| Wavelength $\lambda$ (Å) | 0.9350 | | 0.9312 | | 0.9312 | | 0.9350 | |
| Space group | $P2_12_12_1$ | | $P2_12_12_1$ | | $P2_12_12_1$ | | $P2_12_12_1$ | |
| Unit cell ($a$ Å, $b$ Å, $c$ Å) | 46.75, 71.12, 100.93 | | 46.50, 71.25, 100.99 | | 46.50, 71.07, 100.91 | | 46.66, 71.21, 101.17 | |
| Resolution shell (Å) | 70.71–1.55 | 1.63–1.55 | 57.74–1.30 | 1.37–1.30 | 23.25–1.40 | 1.48–1.40 | 42.26–1.50 | 1.58–1.50 |
| Measurements | 176 037 | 19 544 | 308 677 | 18 087 | 262 663 | 27 072 | 205 116 | 26 399 |
| Average $I/\sigma I$ | 6.8 | 2.2 | 6.5 | 1.7 | 6.2 | 2.8 | 8.2 | 2.0 |
| Unique reflections | 44 320 | 5756 | 78 124 | 8369 | 64 550 | 8960 | 50 504 | 6685 |
| Completeness (%) | 89.8 | 81.6 | 94.1 | 70.6 | 97.4 | 94.0 | 92.5 | 85.4 |
| $R_{merge}$ (%)[a] | 7.6 | 33.3 | 6.2 | 30.2 | 6.3 | 23.4 | 5.2 | 31.5 |
| $R_{cryst}$ (%)[b] | 18.3 | | 18.3 | | 18.2 | | 17.7 | |
| $R_{free}$ (%)[c] | 19.8 | | 19.5 | | 20.3 | | 19.0 | |
| RMS deviation[d] | 0.008 Å (1.78°) | | 0.007 Å (1.68°) | | 0.007 Å (1.85°) | | 0.008 Å (1.87°) | |
| $B$ factors[e] (Å$^2$) | 11.08, 12.53, 9.64, 20.69 | | 11.74, 13.59, 17.78, 21.82 | | 12.15, 14.12, 18.88, 22.20 | | 13.35, 15.02, 19.28, 23.43 | |
| Residues | 328 | | 329 | | 329 | | 329 | |
| Water molecules | 288 | | 446 | | 391 | | 357 | |

[a] $R_{merge} = \Sigma_j \Sigma_h |I_{h,j} - \langle I_h \rangle| / \Sigma_j \Sigma_h \langle I_h \rangle \times 100$.
[b] $R_{cryst} = \Sigma ||F_{obs}| - |F_{calc}|| / \Sigma |F_{obs}| \times 100$.
[c] $R_{free}$ = based on 5% of the total reflections.
[d] RMS deviation from ideality for bonds (followed by the value for angles).
[e] Average $B$ factors in order: main chain, side chain, substrate and solvent.

duced to two molecules of water. However, these results are consistent with the initial involvement of a hydroperoxide–iron–thioaldehyde intermediate in the reaction of IPNS with both AC*O*V and the natural substrate. The techniques employed here allow a more direct observation of enzyme turnover than is possible with incubation studies in solution. They permit structural understanding of how a judiciously perturbed chemical situation prompts the enzyme to selectively redirect the oxidative power of dioxygen along an alternative reaction path.

## 3. Materials and methods

### 3.1. Synthesis of ACOV

The substrate analogue was prepared by caesium carbonate mediated coupling [17] of 2*S*-α-bromoisovaleric acid *tertiary*-butyl ester with the appropriately protected L-α-aminoadipoyl-L-cysteine dipeptide, followed by acid-promoted deprotection [18].

### 3.2. Crystallisation and turnover experiments

Crystals of IPNS:Fe(II):AC*O*V (ca. 0.6×0.2×0.1 mm) were grown under anaerobic conditions as reported previously [10]. For determination of the anaerobic structure, crystals were removed from the anaerobic environment, exchanged into a cryoprotectant buffer (80% crystallisation buffer:20% glycerol) [10] and immediately flash-frozen in liquid nitrogen. Oxygenation experiments were conducted as described previously [4], over reaction times ranging from 20 s to 320 min, at pressures between 20 and 40 bar.

### 3.3. Data collection

Data were collected at 100 K using synchrotron radiation and either a MAR Research CCD camera at beamline ID14-EH3 of the European Synchrotron Radiation Facility (ESRF), Grenoble, France, or an ADSC Quantum4 camera at ESRF beamline ID14-EH4 (Table 1).

### 3.4. Structure determination

Data were processed using MOSFLM [19] and the CCP4 suite of programs [20]. Initial structures were obtained by rigid body refinement of the protein atoms from the IPNS:Fe(II):ACV model [3] against the new data. Model refinement was carried out with REFMAC [20] or SHELXL98 [21]. The final round of refinement for all structures was performed with REFMAC. Restraints for the thiocarboxylate group were calculated from data obtained from the Cambridge Structural Database [22]. The iron–ligand bond lengths were unrestrained throughout refinement. Electron density maps were interpreted using the program O [23]. The iron atom, water molecules, and a sulphate anion (from the crystallisation buffer) were added in the course of refinement. Electron density was clearly visible for substrate-derived species throughout refinement of the respective structures, however substrate or product atoms and adjacent water molecules were only modelled sequentially at advanced stages of refinement. Figures were prepared using the programs BOBSCRIPT [24] and Raster3D [25,26].

## Acknowledgements

We thank V. Lee, R.C. Wilmouth, C.J. Schofield, K.

Harlos, J. Pitt, S. Lee and the scientists at SRS Daresbury, EMBL Hamburg, and ESRF Grenoble for help and discussions. Financial support was provided by the MRC, BBSRC and EPSRC. J.M.O. acknowledges financial support from German BayBFG and DAAD scholarships. P.J.R. was supported by the Rhodes Trust, N.I.B. by a German DAAD fellowship and P.L.R. by the Royal Society.

## References

[1] J.E. Baldwin, C.J. Schofield, The biosynthesis of β-lactams, in: M.I. Page (Ed.), The Chemistry of β-Lactams, Blackie, Glasgow, 1992, pp. 1–78.

[2] J.E. Baldwin, Recent Advances in the Chemistry of β-Lactam Antibiotics, Special Publication No. 52, The Royal Society of Chemistry, London, 1985, pp. 62–85.

[3] P.L. Roach, I.J. Clifton, C.M.H. Hensgens, N. Shibata, C.J. Schofield, J. Hajdu, J.E. Baldwin, Structure of isopenicillin *N* synthase complexed with substrate and the mechanism of penicillin formation, Nature 387 (1997) 827–829.

[4] N.I. Burzlaff, P.J. Rutledge, I.J. Clifton, C.M.H. Hensgens, M. Pickford, R.M. Adlington, P.L. Roach, J.E. Baldwin, The reaction cycle of isopenicillin *N* synthase observed by X-ray diffraction, Nature 401 (1999) 721–724.

[5] J.E. Baldwin, M. Bradley, Isopenicillin *N* synthase: mechanistic studies, Chem. Rev. 90 (1990) 1079–1088.

[6] P.L. Roach, I.J. Clifton, V. Fulop, K. Harlos, G.J. Barton, J. Hajdu, I. Andersson, C.J. Schofield, J.E. Baldwin, Crystal structure of isopenicillin *N* synthase is the first from a new structural family of enzymes, Nature 375 (1995) 700–704.

[7] B.L. Stoddard, New results using Laue diffraction and time-resolved crystallography, Curr. Opin. Struct. Biol. 8 (1998) 612–618.

[8] K. Moffat, Time-resolved crystallography, Acta Crystallogr. A 54 (1998) 833–841.

[9] I. Schlichting, J. Berendzen, K. Chu, A.M. Stock, S.A. Maves, D.E. Benson, B.M. Sweet, D. Ringe, G.A. Petsko, S.G. Sligar, The catalytic pathway of cytochrome P450*cam* at atomic resolution, Science 287 (2000) 1615–1622.

[10] P.L. Roach, I.J. Clifton, C.M.H. Hensgens, N. Shibata, A.J. Long, R.W. Strange, S.S. Hasnain, C.J. Schofield, J.E. Baldwin, J. Hajdu, Anaerobic crystallisation of an isopenicillin *N* synthase·Fe(II)·substrate complex demonstrated by X-ray studies, Eur. J. Biochem. 242 (1996) 736–740.

[11] J.E. Baldwin, G.P. Lynch, C.J. Schofield, Isopenicillin *N* synthase: a new mode of reactivity. J. Chem. Soc. Chem. Commun. (1991) 736–738.

[12] E.L. Hegg, L. Que Jr., The 2-His-1-carboxylate facial triad: an emerging structural motif in mononuclear non-heme iron(II) enzymes, Eur. J. Biochem. 250 (1997) 625–629.

[13] S.L. Lange, L. Que Jr., Oxygen activating nonheme iron enzymes, Curr. Opin. Chem. Biol. 2 (1998) 159–172.

[14] K. Valegård, A.C.T. van Scheltinga, M.D. Lloyd, T. Hara, S. Ramaswamy, A. Perrakis, A. Thompson, H.J. Lee, J.E. Baldwin, C.J. Schofield, J. Hajdu, I. Andersson, Structure of a cephalosporin synthase, Nature 394 (1998) 805–809.

[15] Z. Zhang, J.S. Ren, D.K. Stammers, J.E. Baldwin, K. Harlos, C.J. Schofield, Structural origins of the selectivity of the trifunctional oxygenase clavaminic acid synthase, Nat. Struct. Biol. 7 (1999) 127–133.

[16] L. Serre, A. Sailland, D. Sy, P. Boudec, A. Rolland, E. Pebay-Peyroula, C. Cohen-Addad, Crystal structure of *Pseudomonas fluorescens* 4-hydroxyphenylpyruvate dioxygenase: an enzyme involved in the tyrosine degradation pathway, Struct. Fold. Des. 7 (1999) 977–988.

[17] H.G. Lerchen, H. Kunz, Stereoselective synthesis of D-α-hydroxycarboxylic acid and D-α-hydroxycarboxylic acid-containing depsipeptides in L-amino-acids, Tetrahedron Lett. 26 (1985) 5257–5260.

[18] M. Bodanzky, A. Bodanzky, The practice of peptide synthesis, in: K. Hafner, J.-M. Lehn, C.W. Rees, P.v.R. Schleyer, B.M. Trost, R. Zaradnik (Eds.), Reactivity and Structure Concepts in Organic Chemistry, vol. 21, Springer, Berlin, 1984, pp. 170–173.

[19] A.G.W. Leslie, *Mosflm*, MRC Laboratory of Molecular Biology, Cambridge, 1996.

[20] Collaborative Computational Project No. 4,, The CCP4 suite: programs for protein crystallography, Acta Crystallogr. D 50 (1994) 760–763.

[21] G.M. Sheldrick, T.R. Schneider, SHELXL: high-resolution refinement, Methods Enzymol. 277 (1997) 319–343.

[22] F.H. Allen, O. Kennard, 3D search and research using the Cambridge Structural Database, Chem. Des. Autom. News 8 (1993) 31–37.

[23] T.A. Jones, J.Y. Zou, S.W. Cowan, M. Kjelgaard, Improved methods for building protein models in electron density maps and the location of errors in these models, Acta Crystallogr. A 47 (1991) 110–119.

[24] R.M. Esnouf, Further additions to MolScript version 1.4, including reading and contouring of electron-density maps, Acta Crystallogr. D 55 (1999) 938–940.

[25] E.A. Merrit, M.E.P. Murphy, Raster3D version 2.0: a program for photorealistic molecular graphics, Acta Crystallogr. D 50 (1994) 869–873.

[26] E.A. Merrit, D.J. Bacon, Raster3D: photorealistic molecular graphics, Methods Enzymol. 277 (1997) 505–524.